DOI:
10.1039/C8CP06970K

Document Version
Peer reviewed version

PCCP

Accepted Manuscript

This article can be cited before page numbers have been issued, to do this please use: D. Loru, I. Peña and M. E. Sanz, *Phys. Chem. Chem. Phys.*, 2019, DOI: 10.1039/C8CP06970K.

ROYAL SOCIETY OF CHEMISTRY

rsc.li/pccp

View Article Online
DOI: 10.1039/C8CP06970K

Journal Name

ARTICLE

The role of secondary interactions on the preferred conformers of the fenchone-ethanol complex

Received 00th January 20xx,
Accepted 00th January 20xx

DOI: 10.1039/x0xx00000x

www.rsc.org/

Donatella Loru†[a], Isabel Peña‡[a], M. Eugenia Sanz*[a]

New atomic-level experimental data on the intermolecular non-covalent interactions between a common odorant and a relevant residue at odorant binding sites are reported. The preferred arrangements and binding interactions of fenchone, a common odorant and ethanol, a mimic of serine's side chain, have been unambiguously identified using a combination of high resolution rotational spectroscopy and computational methods. The observed conformers include homochiral (RR) and heterochiral (RS) conformers, with a slight preference for a heterochiral form, and exhibit primary O···H–O hydrogen bonds between fenchone and ethanol. Secondary interactions play a key role in determining the relative configurations of fenchone and ethanol, and in shaping quite a flat potential energy surface, with many conformers close in energy and small barriers for interconversion.

Introduction

The relevance of non-covalent interactions in determining the properties of matter was recognised by J. D. van der Waals in 1873, when he introduced them in his equation of state[1]. Since then, numerous theoretical and experimental studies[2–5] have been devoted to understanding non-covalent interactions and describing their effects in chemistry, physics and biology. Hydrogen bonding, dipole-dipole and dispersion interactions are responsible for the structure of large biomolecules such as DNA and RNA, the physical properties of condensed phases, and the outcome of molecular recognition processes, to cite just a few examples of natural phenomena. They are also important in supramolecular chemistry,[6] where non-covalent synthetic procedures are used to form supramolecular entities.

Small molecular clusters constitute ideal systems for the experimental study of non-covalent interactions, since they can be produced under isolated conditions in supersonic jets and interrogated using gas phase spectroscopic techniques. Model clusters involving water, benzene and noble gases, among others, have been investigated to determine the type of intermolecular interactions involved and their relative importance in dictating the structural arrangement of the cluster components. In particular, rotational spectroscopy is one of the most powerful methods to obtain precise structural information on small biomolecular systems, and it has the advantage of identifying different coexisting conformations, thus showing the system's flexibility (see, for example refs. [7–11]). The development of chirped-pulse Fourier transform microwave (CP-FTMW) spectroscopy[12], which allows fast collection of broad segments of the spectrum at once, facilitating the identification of spectral patterns, has dramatically extended the range and complexity of molecular systems that can be tackled, including large molecules[13], odorants[14,15], and intricate clusters and complexes[16–18].

Here we present the study of the fenchone-ethanol complex using CP-FTMW spectroscopy.[10] Our aim was to start investigating the non-covalent interactions involved in olfaction. Fenchone is a commonly used terpene odorant with a camphoraceous sweet smell, and ethanol acts as a proxy for the side chain of serine, an amino acid proposed to be abundant in odorant binding pockets. Although the structure of odorant binding sites is not known, computational studies suggest that they are likely to be hydrophobic pockets with aliphatic and aromatic amino acids, and an abundance of serine, phenylalanine, isoleucine and leucine[19–25]. However, no experimental data at the atomic level is available on these interactions. By examining complexes of odorants with mimics of amino acid residues we can partially recreate the non-covalent interactions of an odorant at the ligand binding site.

The complex between fenchone and ethanol is an ideal starting point to study non-covalent intermolecular interactions involved in olfaction since fenchone (Fig. 1) is a rigid molecule with only one conformer[10], which removes some of the complexity of the problem. The two lone pairs of the carbonyl oxygen of fenchone are non-equivalent and their

[a] Department of Chemistry, King's College London, SE1 1DB London, UK. E-mail: maria.sanz@kcl.ac.uk. Tel. +44(0)2078487509.
†Present Address: Deutsches Elektronen-Synchrotron (DESY), Notkestraße 85, Geb. 25f / Office 354, D-22607 Hamburg.
‡ Present Address: Departamento de Química Física y Química Inorgánica, Facultad de Ciencias, Universidad de Valladolid, 47011 Valladolid, Spain
Electronic Supplementary Information (ESI) available: [Binding energies, measured frequencies, experimental spectroscopic parameters of the single substituted ^{13}C-ethanol conformers, substitution coordinates and potential energy barriers for the fenchone-ethanol complexes. See DOI: 10.1039/x0xx00000x

interaction with ethanol leads to different conformers of the complex. Ethanol is flexible and can adopt three different conformations, *gauche+* (*g*+), *gauche*– (*g*–) and *trans* (*t*), whether the ∠CCOH dihedral angle assumes a value of +60°, –60° or 180°, respectively (Fig. 2). The two gauche forms of ethanol are equivalent and they interconvert through a tunnelling motion[26]. However, when ethanol interacts with another molecule through a hydrogen bond this tunnelling motion is prevented and the two gauche forms become distinguishable[27–30]. This enables probing of chirality recognition or enantioselectivity, that is, whether there is a preference for forming a homochiral (RR or SS) or a heterochiral (RS or SR) complex. Chirality recognition relies on the concerted effect of several intermolecular interactions, typically including hydrogen bonds, dipole-dipole and dispersion interactions. Our sense of smell rests on interactions between chiral odorants and receptors, and the differences produced by enantioselectivity are sometimes dramatic, with findings of chiral isomers in which one form has a distinct odor quality, whereas the other form is odorless.[31]

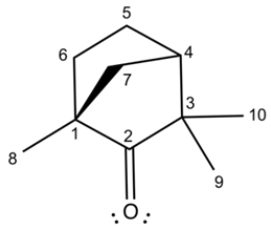

Figure 1. Schematic representation of fenchone showing labelling of carbon atoms.

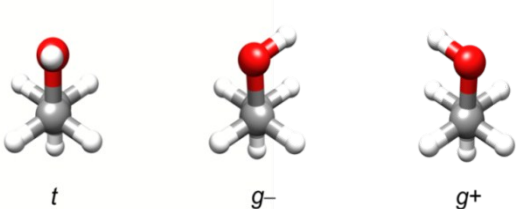

Figure 2. Newman projection of the conformers of ethanol through the C_1–C_2 bond.

We have identified three conformers of fenchone-ethanol by CP-FTMW spectroscopy, where ethanol adopts *g*+ and *g*– conformations. All the complexes show primary O–H···O hydrogen bonds, involving the hydroxyl group of ethanol and the carbonyl oxygen of fenchone, and secondary C–H···O hydrogen bonds between the $–CH_3$ and $–CH_2$ groups of fenchone and the ethanol oxygen. A slight preference for a heterochiral RS configuration has been determined. Secondary weak intermolecular forces have been found to dictate the arrangement of ethanol molecules around fenchone, steering them to specific positions.

Methods

Experimental.

R-Fenchone (98%), absolute ethanol (99%), isotopically enriched 1-^{13}C-ethanol (98%) and enriched 2-^{13}C-ethanol (98%) were purchased from Sigma Aldrich and used without further purification. The rotational spectrum of fenchone-ethanol complexes was recorded with our broadband chirped-pulse rotational spectrometer at King's, which has already been described elsewhere[10,15]. Briefly, a supersonic jet is formed from the expansion of a mixture of fenchone and ethanol seeded into Ne at 6 bar into a vacuum chamber. Molecular collisions at the onset of the supersonic expansion produce the complexes, which are polarised by four chirped microwave pulses spanning 2-8 GHz, spaced 30 μs, and of 4 μs duration. After each microwave pulse, the molecular free induction decay (FID) is collected for 20 μs and it is subsequently transformed to the frequency domain using a fast Fourier transform algorithm. Fenchone is a liquid with a relatively low vapour pressure of 1 mm Hg at 301 K, and it was mildly heated to increase its gas-phase concentration. Optimal spectral intensities of fenchone-ethanol complexes were obtained by placing fenchone in a bespoke heating reservoir, positioned immediately after the nozzle and heated up to *ca.* 350 K, and adding ethanol using a separate external reservoir attached to the injection system. The final spectrum was obtained coherently adding more than 1 million FIDs.

Computational

Theoretical calculations have been performed using the Gaussian09 suite of programs[32] to explore the potential energy surface (PES) of fenchone-ethanol and aid the analysis of the rotational spectrum. The density functional method M062X with the 6-311++G(d,p) basis set was initially used to scan the PES of fenchone-ethanol in steps of 30° along the torsional angles of ethanol and the O–H···O hydrogen bond between fenchone-ethanol (see Figs. S1-S4). The structures of the conformational minima obtained were further optimized using M062X, B3LYP-D3BJ and MP2 methods and the 6-311++G(d,p) basis set allowing all structural parameters to float. Harmonic frequency calculations were carried out on the optimized structures at the corresponding levels of theory to obtain the zero-point corrected electronic energies and confirm that all conformations are real minima in the PES (see Table 1). The binding energies of the conformers have also been calculated at the B3LYP-D3BJ and MP2 levels with the 6-311++G(d,p) basis set, and corrected for the basis set superposition error (BSSE) following the counterpoise procedure[33] and including fragment relaxation terms[34] (see Table S1).

Results

Potential Energy Surface

Fenchone and ethanol are expected to interact through their functional groups and establish an O–H···O hydrogen bond, with the carbonyl group (–C=O) of fenchone acting as a hydrogen bond acceptor and the hydroxyl group of ethanol acting as a hydrogen bond donor. The interaction of ethanol with the two non-equivalent lone pairs of fenchone gives rise to three main relative arrangements of the two moieties, labeled **a**, **b**, and **c**, and depicted in Fig. 3. When ethanol

View Article Online
DOI: 10.1039/C8CP06970K

Journal Name

ARTICLE

Table 1. Calculated spectroscopic parameters at different levels of theory of the twelve lower-energy conformers of fenchone-ethanol within 5.4 kJ mol^{-1}.

	MP2/6-311G++(d,p)			M062X/6-311G++(d,p)			B3LYP-D3BJ/6-311G++(d,p)		
	A/B/C[a]	$\mu_a/\mu_b/\mu_c$[b]	ΔE[c]	A/B/C[a]	$\mu_a/\mu_b/\mu_c$[b]	ΔE[c]	A/B/C[a]	$\mu_a/\mu_b/\mu_c$[b]	ΔE[c]
*t*a1	1175.5/364.2/333.8	3.4/1.1/1.3	0.93	1180.5/376.4/345.2	3.4/1.3/1.3	0.85	1173.4/363.2/332.3	3.6/3.6/1.2	0.95
*t*a2	1201.8/366.9/329.8	3.4/0.3/1.8	0.87	1218.1/370.7/333.2	3.5/0.3/1.4	0.03	1213.0/352.2/315.9	3.3/0.2/0.9	0.45
*g+*a1	1067.1/405.8/372.6	3.3/0.0/1.3	0.48	1070.7/418.9/386.9	3.5/0.3/1.4	0.33	1065.6/404.7/372.1	3.5/0.2/1.3	0.44
*g+*a2	1094.8/408.9/351.1	3.6/0.5/1.5	0.70	1108.9/414.0/356.1	3.7/0.3/1.4	0.37	1106.0/393.9/341.6	3.6/0.3/1.2	0.84
g–a1	1065.9/404.7/356.4	3.6/0.0/1.4	0.87	1068.5/416.5/367.4	3.8/0.2/1.4	0.19	1091.4/389.8/342.0	3.6/0.0/0.9	1.06
g–a2	1099.1/412.7/363.2	3.2/0.6/1.4	0.32	1115.4/420.2/372.6	3.3/0.3/1.5	0.19	1103.1/410.2/361.8	3.4/0.4/1.4	0
*t*b	948.8/451.6/417.5	3.1/0.5/2.0	0.68	942.9/479.5/444.7	3.0/0.4/2.1	2.83	961.3/439.3/406.5	3.4/0.2/2.1	3.07
g+b	921.6/501.0/430.6	3.5/1.1/1.4	0.07	924.2/521.0/446.5	3.5/1.1/1.3	0	916.3/500.2/429.9	3.8/1.1/1.6	2.14
g–b	933.9/484.8/425.8	2.9/1.0/1.3	0	930.7/514.4/447.4	2.8/0.9/1.8	0.86	939.4/474.3/423.2	3.5/0.8/1.5	1.22
*t*c	1012.3/455.8/399.9	1.2/1.1/1.4	2.33	989.0/488.2/432.1	0.5/0.9/1.8	2.56	1024.5/442.1/386.9	1.7/1.1/1.5	5.42
g+c	1013.8/489.8/401.1	3.2/2.0/2.3	2.13	1012.5/517.7/420.9	4.0/1.3/1.9	0.84	1011.0/487.1/398.9	4.1/1.4/1.9	4.49
g–c	1026.9/458.2/399.0	2.8/2.3/2.9	2.67	1025.6/488.9/423.2	4.3/0.8/2.1	1.62	1032.1/439.1/380.5	4.2/1.0/2.0	3.67

[a] *A*, *B* and *C* are the rotational constants in MHz. [b] μ_a, μ_b and μ_c are the absolute values of the electric dipole moment components along the principal inertial axes in Debye. [c] Calculated relative zero-point corrected energies in kJ mol^{-1}.

interacts with the lone pair in *cis* with the two methyl groups attached to C_3 of the fenchone, its OH group is essentially coplanar with OC_2C_1 and equidistant from the two methyl groups (configuration **a**). In contrast, when ethanol interacts with the lone pair in *cis* with the methyl group attached to C_1 of fenchone, the presence of the methyl group causes steric hindrances, giving rise to two different configurations **b** and **c** that correspond to ethanol being on the opposite or same side to bridge carbon C_7, respectively.

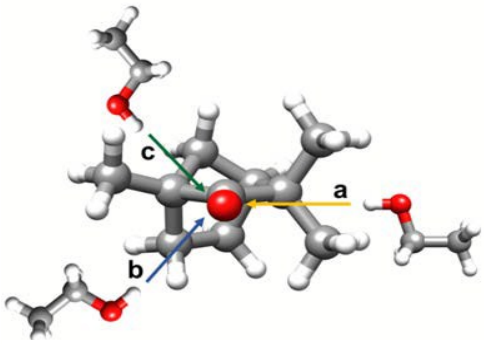

Figure 3. Possible relative configurations of fenchone and ethanol.

Exploration of the PES of the fenchone-ethanol complex revealed 12 distinct minima within 5.4 kJ mol^{-1} originating from the *t*, *g+* and *g–* conformations of ethanol interacting with fenchone in configurations **a**, **b**, and **c** (see Fig. 4). The theoretical spectroscopic parameters and relative energies of the conformers obtained at the different levels of theory are listed in Table 1. Energy differences between the conformers are small (typically within 4.2 kJ mol^{-1}), with conformers

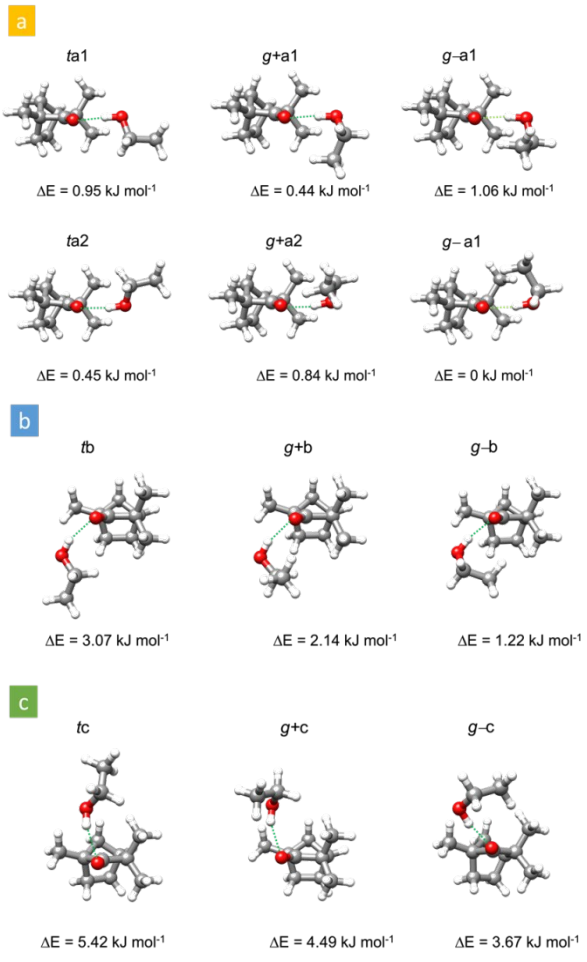

Figure 4. Structures and relative energies, calculated at the B3LYP-D3BJ/6-311++G(d,p) level of theory, of the 12 lower-energy conformers of fenchone-ethanol. The interactions in green represent the primary O-H···O hydrogen bonds established between the carbonyl oxygen in fenchone and the hydroxyl group in ethanol in all the conformers.

View Article Online
DOI: 10.1039/C8CP06970K

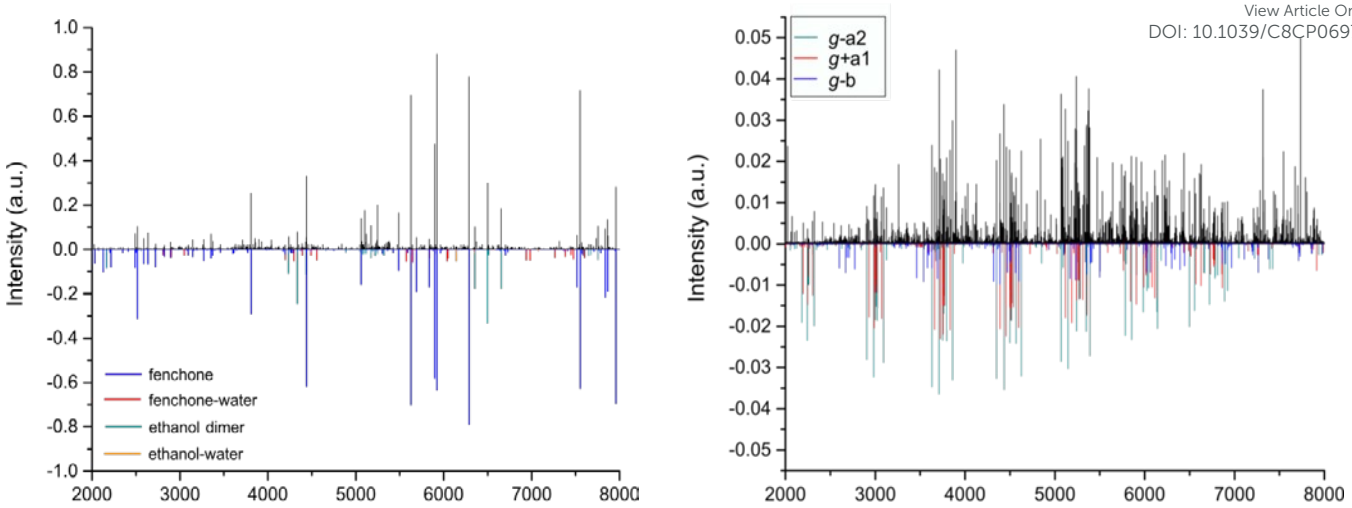

Figure 5. Rotational spectrum of fenchone-ethanol in the 2-8 GHz frequency range. **(left)** Observed spectrum of fenchone-ethanol (upper trace) and simulated spectrum of the already identified species fenchone[23], fenchone-water complexes[42], ethanol dimer[36], ethanol-water complex[41] (lower trace); **(right)** observed spectrum of fenchone-ethanol after removing the lines arising from already identified species (upper trace) and simulated spectrum of the three identified species of fenchone-ethanol (lower trace).

belonging to the **c** family lying at higher energies than conformers belonging to the **a** and **b** families. The complexes involving *trans* ethanol are generally predicted to have higher relative energies and lower binding energies (see Table S1) within each of the **a**, **b**, and **c** families by the different methods used. There is no consensus on which conformer is the global

minimum among the methods used: it is predicted as conformer ***g*–b** by MP2, isomer ***g*+b** by M062X and isomer ***g*–a2** by B3LYP-D3BJ. All conformers are predicted to have geometries close to the symmetric prolate limit, and their rotational constants can be roughly grouped into three different families according to the three main configurations **a**, **b** and **c**. Rotational constants within each configuration are very similar.

Conformers belonging to each of **a**, **b**, and **c** families with different ethanol conformations are separated by low interconversion barriers of 4-5 kJ mol^{-1} (see Figure S1-S4). Interestingly, when the torsional angle corresponding to the O–H···O hydrogen bond is scanned, there is a clearly preferred relative arrangement of ethanol and fenchone for configurations **b** and **c**. For configuration **a**, on the contrary, the potential energy surface is very flat over a 180° range where two different conformations of fenchone-ethanol are found as minima, with very close energies and conformational interconversion barriers of *ca*. 1.2 kJ mol^{-1} (see Figs. S2-S4).

Rotational Spectrum: Analysis and Conformational Identification

On first inspection the broadband rotational spectrum of fenchone-ethanol in the 2-8 GHz range seems to contain just a few hundred lines corresponding to several species previously identified, including bare fenchone[10], ethanol dimer[30], ethanol-water[35], and fenchone-water complexes[36] (see Fig. 5 (left)). Once these lines are removed, whole new series of lines of lower intensity are revealed (see Fig. 5 (right)). Some of the lines are bunched together showing the pattern expected for the J+1 ← J *a*-type transitions of a species close to a prolate symmetric top limit, where J is the rotational quantum number. Three distinct *a*-type spectra corresponding to three different conformers of fenchone-ethanol were identified. Fits of initial sets of *a*-type transitions measured for each conformer yielded preliminary rotational constants that were then used to predict and measure more transitions. All the measured transitions were fit using the Watson Hamiltonian in the A reduction and I^r representation[37] and Pickett's program[38], and are listed in Tables S2-S4 of the Supplementary Information. The experimentally determined rotational constants and centrifugal distortion constants for the three conformers of fenchone-ethanol are listed in Table 2.

Assignment of each observed fenchone-ethanol conformer to a particular species is accomplished by comparing the theoretical and experimental structural data. From the values of the theoretical and experimental rotational constants (see Tables 1 and 2), it can be concluded that conformer **III** belongs to the **b** family, while conformers **I** and **II** belong to the **a** family. However, the close values of the predicted rotational constants preclude a conclusive identification. To unambiguously assign conformers **I** and **II** to a specific structure and to confirm the observed conformers to a specific structure, it is necessary to determine the location of ethanol in each conformer of the complex. This was done by conducting further experiments using isotopically enriched samples of $^{13}C_1$- and $^{13}C_2$-ethanol, and calculating the *a*, *b*, and *c* coordinates of the C_1 and C_2 atoms of ethanol from the rotational constants of the corresponding isotopologues (Tables S5-S12) applying Kraitchman's equations[39,40]. By comparing the experimentally determined coordinates and the theoretical ones (Tables S13 and S14), conformers **I**, **II** and **III** are unambiguously assigned as conformers ***g*+a1**, ***g*–a2** and ***g*–b**, respectively. Considering these assignments, the best performing theoretical method used is B3LYP-D3BJ, which yields the closest values of the theoretical rotational constants to the experimental ones. A graphical comparison of B3LYP-

View Article Online
DOI: 10.1039/C8CP06970K

Table 2 Experimental spectroscopic parameters of the three observed conformers of fenchone-ethanol.

	I	II	III
A (MHz)[a]	1076.9231(44)[e]	1106.6954(12)	930.714(17)
B (MHz)	392.49827(55)	398.85708(29)	476.94132(41)
C (MHz)	357.88554(48)	352.22739(33)	419.31310(46)
Δ_J (kHz)	0.2510(26)	0.1169(24)	0.1225(27)
Δ_{JK} (kHz)	0.296(17)	0.186(28)	0.129(22)
δ_J (kHz)	-0.0423(14)	-	-
Δ_K (kHz)	1.11(17)	-	-
a/*b*/*c*[b]	y/n/y	y/n/y	y/n/n
N[c]	62	45	43
σ (kHz)[d]	6	8	8

[a] A, B and C are the rotational constants. Δ_J, Δ_{JK}, and δ_J are the centrifugal distortion constants. [b] *a*, *b* and *c* represent the type of transitions observed in the rotational spectrum, yes (y) or no (n). [c] N is the number of the fitted transitions. [d] σ is the rms deviation of the fit. [e] Standard error in parentheses in units of the last digit

D3BJ and substitution coordinates for the three fenchone-ethanol conformers is displayed in Figure 6.

The relative conformational abundances of the observed conformers were estimated by measuring the intensities of a set of common *a*-type transitions and normalising them by the square of the dipole moment component μ_a (as in our experiment line intensity is proportional to μ_i^2).[12] The relative abundances were found to be ***g*–a2** > ***g*+a1**> ***g*–b** = 1 > 0.7 >0.5

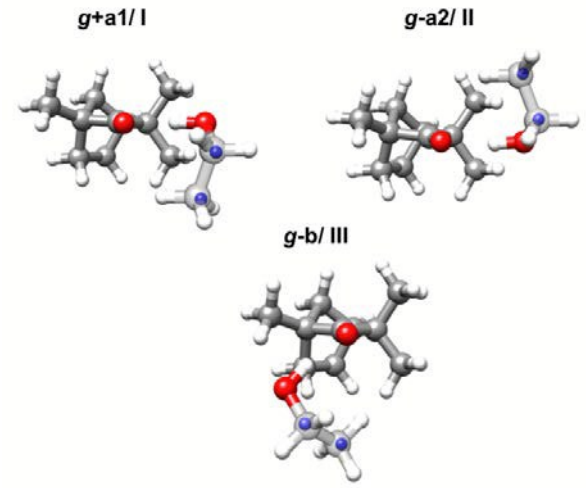

Figure 6. Comparison between the theoretical structures of conformers **g–a2, g+a1** and **g–b** calculated at the B3LYP-D3BJ/6-311++G(d,p) level of theory with the substitution coordinates calculated for the carbons of ethanol represented as blue spheres.

in agreement with the predicted zero-point corrected energies for the conformers at the B3LYP-D3BJ/6-311++G(d,p) level. Our observations are also consistent with calculated binding energies by MP2 and B3LYP-D3BJ methods (Table S1).

Discussion

The three observed fenchone-ethanol conformers show a primary O–H···O hydrogen bond with the hydroxyl group of ethanol as hydrogen donor and the carbonyl oxygen of fenchone as hydrogen acceptor. Theoretically calculated C–H···O interactions range between 2.48-2.62 Å (B3LYP-D3BJ) and 2.52-2.65 Å (MP2), well below the sum of the van der Waals radii of carbon and oxygen (2.72 Å)[41]. This indicates that additional secondary C–H···O hydrogen bonds are established. The establishment of secondary interactions is also reflected in the non-collinear arrangement of the O–H···O atoms, with values (B3LYP-D3BJ) of 170.9° for ***g*–a2,** 172.9° for ***g*+a1,** and 163.6° for ***g*–b**. Deviation of hydrogen bonds from collinearity has been related to the establishment of secondary interactions for a range of complexes[42,43].

In all the observed conformers of the complex ethanol is in a *gauche* configuration, which favours intermolecular C–H···O secondary hydrogen bonds and dispersion interactions.[44] The balance between intra- and intermolecular forces drives ethanol to change its conformational preferences from the *trans* conformer preferred in bare ethanol[26]. This change has also been observed in other complexes of ethanol where secondary interactions are established in addition to the primary hydrogen bond[28,29,27,30,35]. In complexes where there are no secondary interactions the preference for *trans* ethanol is maintained[45].

The most abundant conformers of fenchone-ethanol observed, ***g*+a1** and ***g*–a2**, belong to the **a** family, where the O–H···O hydrogen bond is on the same plane as the carbonyl oxygen lone pair. This arrangement maximises the overlap between the lone pair electronic density and the hydrogen atom, explaining the clear preference for the **a** configuration. In the **b** and **c** configurations a similar coplanar arrangement is prevented by the presence of a methyl group at C_1 of fenchone, which makes these configurations less energetically favourable, and rationalises the lower abundance of conformer ***g*–b**. Symmetry adapted perturbation theory (SAPT)[46,47] has been used to get further insight into the interactions established between the two moieties in the complexes (Table 3). The electrostatic contribution to the total energy is smaller for the ***g*–b** conformer than for ***g*+a1** and ***g*–a2**, reflecting the imperfect overlap of the lone pair of the

View Article Online
DOI: 10.1039/C8CP06970K

Table 3. Binding energy decomposition (SAPT(0)/jun-cc-pDVZ) in kJmol^{-1} for the observed conformers of fenchone-ethanol.

	$\Delta E_{electrostatic}$	$\Delta E_{exchange}$	$\Delta E_{induction}$	$\Delta E_{dispersion}$	ΔE_{total}
g+a1	-53.8	54.7	-16.9	-19.6	-35.5
g−a2	-54.3	55.4	-17.1	-19.8	-35.8
g−b	-47.9	51.0	-15.0	-21.7	-33.6

oxygen in fenchone and the hydrogen atom of the hydroxyl group. The relative contribution of the electrostatic and dispersion terms varies between conformers, with dispersion terms being similar in ***g+*a1** and ***g*–a2** (about 36% of the electrostatic terms) and larger in ***g*–b** (about 45% of the electrostatic term)**.** The lower contribution of the electrostatic terms to the overall energy in ***g*–b** is consistent with the longer distance of its O–H···O hydrogen bond predicted by B3LYP-D3BJ, of 1.91 Å for ***g*–b** in comparison with 1.87 Å for ***g+*a1** and ***g*–a.**

Primary O–H···O hydrogen bond lengths for the different conformers are predicted in an extremely consistent manner by the different theoretical methods used. MP2 for example, predicts them longer by 0.03-0.04 Å than B3LYP-D3BJ, but both methods predict the same variation between conformers. Secondary interactions, on the contrary, are estimated differently for the various conformers by the different methods, with variations in the range 0.04-0.11 Å between MP2 and B3LYP-D3BJ. Differences in estimating secondary interactions are very likely to be related to the different conformational energy orderings predicted by the computational methods used.

The estimated relative abundances of the observed conformers of fenchone-ethanol, ***g*–a2** > ***g+*a1** > ***g*–b** = 1 > 0.7 > 0.5, show a small preference of R-fenchone to interact with *g*–ethanol, which corresponds to S-ethanol following IUPAC nomenclature[48]. Therefore, we can conclude that the heterochiral RS fenchone-ethanol conformer ***g*–a2** is slightly preferred over the homochiral RR one, ***g+*a1**. The small prevalence of the RS complex is due to the minor differences in the secondary interactions (C–H···O hydrogen bonds and dispersion forces), as primary hydrogen bond lengths and angles are predicted to be the same for both RS and RR complexes. The C–H···O hydrogen bonds in ***g*–a2** are slightly shorter (2.58 Å and 2.55 Å) than those in ***g+*a1** (2.62 Å and 2.53 Å).

Secondary interactions have been revealed to play a decisive role in determining the relative arrangement of fenchone and ethanol. Steric hindrance due to the presence of a methyl group at C_1 of fenchone steers ethanol to a precise location above or below the plane defined by $\angle C_1C_2OC_3$ of fenchone when ethanol interacts with the oxygen lone pair in *cis* with C_1 (**b** and **c** configurations). Strikingly, interactions of ethanol with the oxygen lone pair in *trans* to C_1 exhibit a remarkable indifference to the orientation of ethanol (**a** configurations, see Figs. S2-S4). In the latter, secondary interactions between ethanol and fenchone are very similar irrespective of the orientation of ethanol, and therefore, once the primary hydrogen bond is established, fenchone does not show a preference in its arrangement with respect to ethanol.

At the odorant receptor binding site, several residues (probably hydrophobic) would interact with fenchone in addition to a $–CH_2OH$ side chain. Hydrogen bond interactions of fenchone with a $–CH_2OH$ side chain through **a** configurations will be favoured, but once the primary hydrogen bond is established, accommodation of fenchone in the binding pocket will be directed by interactions with other residues. Our data suggest that different arrangements of fenchone with close energies are possible, as the PES of fenchone-ethanol is relatively flat, with small energy differences between conformers and low interconversion barriers. This indicates that conformational interconversion is reasonably easy and several conformations are accessible, which alludes to fenchone's capacity to interact with multiple receptor sites.

Conclusions

The conformational landscape of fenchone-ethanol has been fully characterised, and three different conformers have been identified using CP-FTMW spectroscopy. The experimental results have allowed us to benchmark theoretical methods and to discover the important role played by secondary interactions, which drive the relative arrangement of the two moieties and the slight preference for the heterochiral conformer. The local environment in the receptor binding site will be crucial in modulating the ultimate location of fenchone with respect to the $–CH_2OH$ side chain of the amino acid serine. The flexibility of the side chain and the relatively flat potential energy surface point to a range of possible arrangements in receptor binding sites with small energy differences.

Our understanding of the interplay between the various intermolecular forces that shape the three-dimensional structure of clusters is still limited. Rotational spectroscopy, with its inherent high resolution and structural discrimination, has proved to be a very valuable tool to gain insight on non-covalent interactions. Further rotational studies, increasing the number of binding partners or looking at binding partners with more points of contact, could shed more light on the role of the different non-covalent interactions and help describe fundamental chemical, physical, and biochemical processes from a molecular point of view.

DOI: 10.1039/C8CP06970K

Conflicts of interest

There are no conflicts to declare.

Acknowledgements

The authors would like to thank funding from the EU FP7 (Marie Curie grant PCIG12-GA-2012-334525) and King's College London.

References

1 J. D. van der Waals, Leiden, 1873.

2 K. Müller-Dethlefs and P. Hobza, Noncovalent Interactions: A Challenge for Experiment and Theory, *Chem. Rev.*, 2000, **100**, 143–168.

3 P. A. Kollman, Noncovalent Interactions, *Acc. Chem. Res.*, 1977, **10**, 365–371.

4 K. R. Leopold, G. T. Fraser, S. E. Novick and W. Klemperer, Current Themes in Microwave and Infrared Spectroscopy of Weakly Bound Complexes, *Chem. Rev.*, 1994, **94**, 1807–1827.

5 A. C. Legon and D. J. Millen, Directional character, strength, and nature of the hydrogen bond in gas-phase dimers, *Acc. Chem. Res.*, 1987, **20**, 39–46.

6 J.-M. Lehn, Supramolecular Chemistry-Scope and Perspectives. Molecules, Supermolecules, and Molecular Devices (Novel Lecture), *Angew. Chem. Int. Ed. Engl.*, 1988, **27**, 89–112.

7 Z. Kisiel, O. Desyatnyk, E. Białkowska-Jaworska and L. Pszczółkowski, The structure and electric dipole moment of camphor determined by rotational spectroscopyElectronic supplementary information (ESI) available: Measured and fitted frequencies of field-free rotational transitions and of Stark components, and the results of fitting the molecular geometry. See http://www.rsc.org/suppdata/cp/b2/b212029a/, *Phys. Chem. Chem. Phys.*, 2003, **5**, 820–826.

8 M. Chrayteh, P. Dréan and T. R. Huet, Structure determination of myrtenal by microwave spectroscopy and quantum chemical calculations, *J. Mol. Spectrosc.*, 2017, **336**, 22–28.

9 H. Mouhib, W. Stahl, M. Lüthy, M. Büchel and P. Kraft, Cassis Odor through Microwave Eyes: Olfactory Properties and Gas-Phase Structures of all the Cassyrane Stereoisomers and its Dihydro Derivatives, *Angew. Chemie Int. Ed.*, 2011, **50**, 5576–5580.

10 D. Loru, M. A. Bermúdez and M. E. Sanz, Structure of fenchone by broadband rotational spectroscopy, *J. Chem. Phys.*, 2016, **145**, 074311.

11 S. R. Domingos, C. Pérez, C. Medcraft, P. Pinacho and M. Schnell, Flexibility unleashed in acyclic monoterpenes: conformational space of citronellal revealed by broadband rotational spectroscopy, *Phys. Chem. Chem. Phys.*, 2016, **18**, 16682–16689.

12 G. G. Brown, B. C. Dian, K. O. Douglass, S. M. Geyer, S. T. Shipman and B. H. Pate, A broadband Fourier transform microwave spectrometer based on chirped pulse excitation, *Rev. Sci. Instrum.*, 2008, **79**, 1–13.

13 A. A. Fokin, T. S. Zhuk, S. Blomeyer, C. Pérez, L. V. Chernish, A. E. Pashenko, J. Antony, Y. V. Vishnevskiy, R. J. F. Berger, S. Grimme, C. Logemann, M. Schnell, N. W. Mitzel and P. R. Schreiner, Intramolecular London Dispersion Interaction Effects on Gas-Phase and Solid-State Structures of Diamondoid Dimers, *J. Am. Chem. Soc.*, 2017, **139**, 16696–16707.

14 A. Krin, C. Pérez, P. Pinacho, M. M. Quesada-Moreno, J. J. López-González, J. R. Avilés-Moreno, S. Blanco, J. C. López and M. Schnell, Structure Determination, Conformational Flexibility, Internal Dynamics, and Chiral Analysis of Pulegone and Its Complex with Water, *Chem. - A Eur. J.*, 2018, **24**, 721–729.

15 D. Loru, M. M. Quesada-Moreno, J. R. Avilés-Moreno, N. Jarman, T. R. Huet, J. J. López-González and M. E. Sanz, Conformational Flexibility of Limonene Oxide Studied By Microwave Spectroscopy, *ChemPhysChem*, 2017, **18**, 268.

16 C. Pérez, M. T. Muckle, D. P. Zaleski, N. A. Seifert, B. Temelso, G. C. Shields, Z. Kisiel and B. H. Pate, Structures of Cage, Prism, and Book Isomers of Water Hexamer from Broadband Rotational Spectroscopy, *Science (80-.).*, 2012, **336**, 897–902.

17 N. A. Seifert, A. L. Steber, J. L. Neill, C. Pérez, D. P. Zaleski, B. H. Pate and A. Lesarri, The interplay of hydrogen bonding and dispersion in phenol dimer and trimer: structures from broadband rotational spectroscopy, *Phys. Chem. Chem. Phys.*, 2013, **15**, 11468.

18 C. Pérez, D. P. Zaleski, N. A. Seifert, B. Temelso, G. C. Shields, Z. Kisiel and B. H. Pate, Hydrogen bond cooperativity and the three-dimensional structures of water nonamers and decamers, *Angew. Chemie - Int. Ed.*, 2014, **53**, 14368–14372.

19 G. Launay, G. Sanz, E. Pajot-Augy and J. F. Gibrat, Modeling of mammalian olfactory receptors and docking of odorants, *Biophys. Rev.*, 2012, **4**, 255–269.

20 Y. Pilpel and D. Lancet, The variable and conserved interfaces of modeled olfactory receptor proteins., *Protein Sci.*, 1999, **8**, 969–977.

21 K. Khafizov, C. Anselmi, A. Menini and P. Carloni, Ligand specificity of odorant receptors, *J. Mol. Model.*, 2007, **13**, 401–409.

22 S. E. Hall, W. B. Floriano, N. Vaidehi and W. A. Goddard, Predicted 3-D structures for mouse 17 and rat 17 olfactory receptors and comparison of predicted odor recognition profiles with experiment, *Chem. Senses*, 2004, **29**, 595–616.

23 S. Katada, Structural Basis for a Broad But Selective Ligand Spectrum of a Mouse Olfactory Receptor: Mapping the Odorant-Binding Site, *J. Neurosci.*, 2005, **25**, 1806–1815.

24 O. Baud, S. Etter, M. Spreafico, L. Bordoli, T. Schwede, H. Vogel and H. Pick, The Mouse Eugenol Odorant Receptor: Structural and Functional Plasticity of a Broadly Tuned Odorant Binding Pocket, *Biochemistry*, 2011, **50**, 843–853.

25 G. Launay, S. Téletchéa, F. Wade, E. Pajot-Augy, J.-F. Gibrat and G. Sanz, Automatic modeling of mammalian olfactory

receptors and docking of odorants, *Protein Eng. Des. Sel.*, 2012, **25**, 377–386.

26 J. C. Pearson, K. V. L. N. Sastry, E. Herbst and F. C. De Lucia, The Millimeter- and Submillimeter-Wave Spectrum of Gauche-Ethyl Alcohol, *J. Mol. Spectrosc.*, 1996, **175**, 246–261.

27 N. Borho and Y. Xu, Lock-and-key principle on a microscopic scale: The case of the propylene oxide···ethanol complex, *Angew. Chemie - Int. Ed.*, 2007, **46**, 2276–2279.

28 N. Borho and Y. Xu, Molecular recognition in 1 : 1 hydrogen-bonded complexes of oxirane and trans-2,3-dimethyloxirane with ethanol: a rotational spectroscopic and ab initio study., *Phys. Chem. Chem. Phys.*, 2007, **9**, 4514–20.

29 Q. Gou, L. B. Favero, G. Feng, L. Evangelisti, C. Pérez and W. Caminati, Interactions between Ketones and Alcohols: Rotational Spectrum and Internal Dynamics of the Acetone–Ethanol Complex, *Chem. - A Eur. J.*, 2017, **23**, 11119–11125.

30 D. Loru, I. Peña and M. E. Sanz, Ethanol dimer: Observation of three new conformers by broadband rotational spectroscopy, *J. Mol. Spectrosc.*, 2017, **335**, 93–101.

31 D. P. Simmons, D. Reichlin, D. Skuy and C. Margot, Stereoselectivity of odor perception: odorless enantiomers of strong perfumes, *Chem. Senses*, 1992, **17**, 881.

32 M. J. Frisch, G. W. Trucks, H. B. Schlegel, G. E. Scuseria, M. A. Robb, J. R. Cheeseman, G. Scalmani, V. Barone, B. Mennucci, G. A. Petersson, H. Nakatsuji, M. Caricato, X. Li, H. P. Hratchian, A. F. Izmaylov, J. Bloino, G. Zheng, J. L. Sonnenberg, M. Hada, M. Ehara, K. Toyota, R. Fukuda, J. Hasegawa, M. Ishida, T. Nakajima, Y. Honda, O. Kitao, H. Nakai, T. Vreven, J. Montgomery, J. A., J. E. Peralta, F. Ogliaro, M. Bearpark, J. J. Heyd, E. Brothers, K. N. Kudin, V. N. Staroverov, R. Kobayashi, J. Normand, K. Raghavachari, A. Rendell, J. C. Burant, S. S. Iyengar, J. Tomasi, M. Cossi, N. Rega, J. M. Millam, M. Klene, J. E. Knox, J. B. Cross, V. Bakken, C. Adamo, J. Jaramillo, R. Gomperts, R. E. Stratmann, O. Yazyev, A. J. Austin, R. Cammi, C. Pomelli, J. W. Ochterski, R. L. Martin, K. Morokuma, V. G. Zakrzewski, G. A. Voth, P. Salvador, J. J. Dannenberg, S. Dapprich, A. D. Daniels, Ö. Farkas, J. B. Foresman, J. V. Ortiz, J. Cioslowski and D. J. Fox, *Gaussian 09, Revision E. 01; Gaussian*, 2009.

33 S. F. Boys and F. Bernardi, The calculation of small molecular interactions by the differences of separate total energies. Some procedures with reduced errors, *Mol. Phys.*, 1970, **19**, 553–566.

34 S. S. Xantheas, On the importance of the fragment relaxation energy terms in the estimation of the Basis Set Superposition Error correction to the intermolecular interaction energy, *J. Chem. Phys.*, 1996, **104**, 8821–8824.

35 I. A. Finneran, P. B. Carroll, M. A. Allodi and G. A. Blake, Hydrogen bonding in the ethanol–water dimer, *Phys. Chem. Chem. Phys.*, 2015, **17**, 24210–24214.

36 M. Chrayteh, P. Drean, T. Huet, D. Loru and M. Sanz, in *The 25th Colloquium on High-Resolution Molecular Spectroscopy, HRMS*, Helsinki, Finland, 2017.

37 J. K. G. Watson, in *Vibrational spectra and structure, vol 6 A series of advances*, 1977, pp. 1–89.

38 H. M. Pickett, The fitting and prediction of vibration-rotation spectra with spin interactions, *J. Mol. Spectrosc.*, 1991, **148**, 371–377.

39 J. Kraitchman, Determination of Molecular Structure from Microwave Spectroscopic Data, *Am. J. Phys.*, 1953, **21**, 17–24.

40 Z. Kisiel, PROSPE-Programs for Rotational spectroscopy, *Spectrosc. from Sp.*, 2001, 91–106.

41 A. Bondi, Van der waals volumes and radii, *J. Phys. Chem.*, 1964, **68**, 441–451.

42 A. C. Legon, Non-linear hydrogen bonds and rotational spectroscopy: Measurement and rationalisation of the deviation from linearity, *Faraday Discuss.*, 1994, **97**, 19–33.

43 M. E. Sanz, A. Lesarri, J. C. Lopez and J. L. Alonso, Hydrogen bond in molecules with large-amplitude motions: A rotational study of trimethylene sulfide···HCl, *Angew. Chemie - Int. Ed.*, 2001, **40**, 935–938.

44 J. P. Wagner and P. R. Schreiner, London Dispersion in Molecular Chemistry - Reconsidering Steric Effects, *Angew. Chemie - Int. Ed.*, 2015, **54**, 12274–12296.

45 B. M. Giuliano, L. B. Favero, A. Maris and W. Caminati, Shapes and internal dynamics of the 1:1 adducts of ammonia with trans and gauche ethanol: A rotational study, *Chem. - A Eur. J.*, 2012, **18**, 12759–12763.

46 B. Jeziorski, R. Moszynski and K. Szalewicz, Perturbation Theory Approach to Intermolecular Potential Energy Surfaces of van der Waals Complexes, *Chem. Rev.*, 1994, **94**, 1887–1930.

47 R. M. Parrish, L. A. Burns, D. G. A. Smith, A. C. Simmonett, A. E. DePrince, E. G. Hohenstein, U. Bozkaya, A. Y. Sokolov, R. Di Remigio, R. M. Richard, J. F. Gonthier, A. M. James, H. R. McAlexander, A. Kumar, M. Saitow, X. Wang, B. P. Pritchard, P. Verma, H. F. Schaefer, K. Patkowski, R. A. King, E. F. Valeev, F. A. Evangelista, J. M. Turney, T. D. Crawford and C. D. Sherrill, Psi4 1.1: An Open-Source Electronic Structure Program Emphasizing Automation, Advanced Libraries, and Interoperability, *J. Chem. Theory Comput.*, 2017, **13**, 3185–3197.

48 IUPAC, *Compendium of Chemical Terminology*, 2014.